Rotating Spiral Waves Created by Geometry

Konstantin Agladze, James P. Keener,* Stefan C. Müller, Alexander Panfilov

The Belousov-Zhabotinsky reagent and numerical simulations were used to show that under high-frequency stimuli, rotating spiral waves can be initiated in a homogeneous excitable medium in the vicinity of domain boundaries or inexcitable barriers with sharp corners.

Rotating spiral waves, also known as rotors (*1*) or vortices (*2*), occur in a variety of nonlinear excitable media. Biological examples of such media include populations of *Dictyostelium discoideum* amoebae (*3*), retina (*4*), heart tissue (*5*), and *Xenopus* oocytes (*6*). In physicochemical systems, spiral waves have been observed in oscillating reactions (*1, 7*) and heterogeneous catalysis (*8*).

The appearance and multiplication of spiral waves disorder the spatial organization of the medium and may result in turbulent or chaotic behavior (*9*). For nearly 30 years the only reasonable explanation of spontaneous spiral wave initiation confirmed in a variety of excitable tissue was that it is due to heterogeneity of refractoriness (*10*); that is, spatial differences in recovery properties of the tissue can lead to localized failure of propagation and subsequent curl-up into spiral waves.

We verified the possibility of a mechanism for generation of spiral waves under high-frequency forcing, having observed it both computationally and experimentally in Belousov-Zhabotinsky (BZ) reagent. These spirals are the result of the interaction of waves with inexcitable obstacles or domain boundaries in an otherwise homogeneous medium. The mechanism of formation is quite general: it is the result of generic properties of excitable media including the dependence of wavefront velocity on the local wave frequency and the wavefront curvature. The simple criteria for the appearance of spirals are (i) the frequency of the periodic wave train must be above some critical frequency and (ii) the domain wall or obstacle must have sharp corners. Though this phenomenon is visually similar to vortex formation in hydrodynamical turbulence, it occurs here in the absence of physical mass-transfer and by a different mechanism.

Multiple rotors found in simulations of an excitable medium with randomly located inexcitable obstacles are shown in Fig. 1A. For this simulation, we initiated a train of periodic waves, which propagated from bottom to top in the frame. The sequence of events at each obstacle is similar, so Fig. 1, B and C, show what happens at a single obstacle. Starting from rest, waves subsequent to the first travel with slowed velocity because of incomplete recovery. The wavelength between successive waves becomes shorter and the frequency becomes higher, asymptotically approaching the frequency of stimulus (which is fixed). When the local period is relatively long so that the medium at the obstacle is well recovered (Fig. 1B), the wave splits at the obstacle into two waves with free ends, each of which circumnavigate the obstacle. Behind the obstacle the two wave ends meet and once again form a single wavefront. The remaining influence of the obstacle is a nonplanar deformation of the reconnected wavefront, the amplitude of which decreases with distance from the obstacle and eventually disappears (because of the curvature influence on wavefront velocity). As the local wave period becomes shorter, the wave tips meet each other at an increased distance from the obstacle, and the disturbance to the reconnected wavefront behind the obstacle is more pronounced. When the local period becomes shorter than some critical value, the wave splits and the ends remain separated from the obstacle and from each other (Fig. 1C). When the externally applied stimulation is stopped, a pair of counterrotating spiral waves remains in the medium. If there are many obstacles or domain wall corners, as in Fig. 1A, there are many spirals rotating in the medium.

The necessary conditions for the initiation of spirals by this mechanism are external stimuli of sufficiently high frequency and obstacles with sufficient size and sufficiently sharp corners. In our simulations, at an obstacle with a 90° corner, spirals were formed if the period of external stimulation was less than 0.87 times the period of spiral wave rotation (but longer than the absolute refractory period of the medium) and if the obstacle length was larger than 0.10 to 0.15 λ, where λ is the spiral wavelength. As the turning angle increases (turning angle = angle between boundary normal vectors before and after the corner), the frequency threshold for rotor formation decreases. In our computations, the critical period for a turning angle of 180° (the largest possible turning angle) was 0.95 times the rotor period.

Wave propagation around a boundary corner as found in experiments with the BZ reaction is shown in Fig. 2. A layer of 2% agarose gel (0.7 mm thick) was prepared to serve as a matrix for the medium. The use of a gel avoids hydrodynamic disturbances and allows the boundary geometry to be created by cutting a sharp corner into the gel layer. After a rectangular portion of the gel was removed, the gel was soaked for 10 min in the BZ medium. The aqueous solution was then removed, especially carefully at the corner (which must remain sharp). To prevent the gel surface from drying and to decrease the influence of oxygen on the reaction, we covered the gel with a 2-mm layer of transparent, colorless silicon oil. Waves were initiated in the medium by touching the gel layer with a silver wire (diameter, 0.5 mm). Spiral waves were used as permanent wave sources. To create a wave source with a frequency higher than that of the usual spiral wave, we injected with a syringe a microdrop (about 10 μl) of 0.15 M sulfuric acid into the core of a chosen spiral wave, thereby increasing its frequency of rotation. Later, to decrease the frequency of or kill the spiral source, we used microdrops of 1 M bromide solution (*2, 11*), as this is known to inhibit the BZ reaction.

When the frequency of the waves was less than or equal to the normal rate of spiral rotation, waves moved around the corner without noticeable wave breaks (Fig. 2, A to D). When the local frequency was increased above the critical value, a wave break appeared spontaneously (Fig. 2D). In time the wave break evolved into a rotating spiral (Fig. 2, E and F). Because the frequency of forcing was higher than the natural frequency of the spiral (*11*), the spiral drifted away from its point of origin (to the right in this experiment, not shown).

The initiation of spirals at short time intervals and at large magnification is shown in Fig. 2. Figure 3 documents the phenomenon over a longer period of time and illustrates the evolution and stability of a fully developed spiral that survives after the stimulation has been switched off. Figure 3 also shows spiral wave origination at a sharp 90° corner cut into a millipore filter which was used as a support for the BZ

K. Agladze, Institute of Theoretical and Experimental Biophysics, Russian Academy of Sciences, Pushchino, Moskow Region, 142292, Russia.
J. P. Keener, Department of Mathematics, University of Utah, Salt Lake City, UT 84112, USA.
S. C. Müller, Max-Planck-Institute für Ernährungsphysiologie, Rheinlanddamm 201, 4600 Dortmund, Germany.
A. Panfilov, Bioinformatica, University of Utrecht, Padualaan 8, 3584 CH Utrecht, Netherlands.

*To whom correspondence should be addressed.

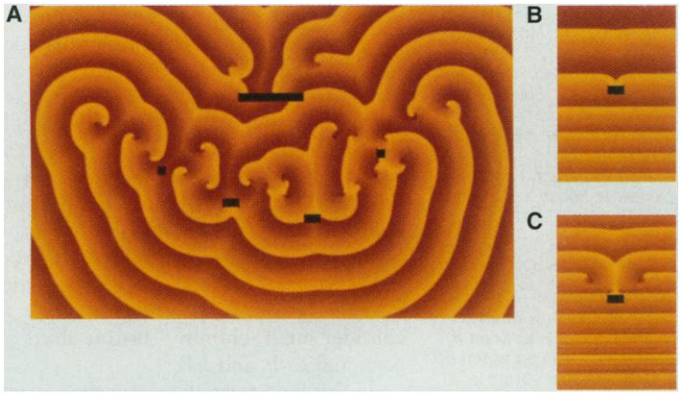

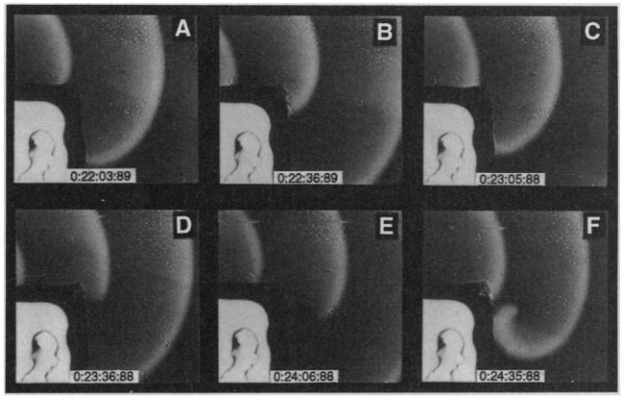

Fig. 1 (left). Rotors resulting from high-frequency stimuli in an excitable medium with obstacles. (**A**) The wave pattern that results at t = 930 (time units) in an excitable medium of 600 by 400 grid points containing five randomly distributed obstacles under high-frequency stimulation with period 11.5 time units, applied before t = 650. (**B** and **C**) The wave pattern at a single obstacle under the same conditions as in (A) at t = 120 (B) and t = 240 (C). For details of the computations see (*18*). **Fig. 2 (right).** Spiral wave origination in an agarose gel soaked with BZ reagent with the following concentrations: $NaBrO_3$, 0.16 M; H_2SO_4, 0.33 M; $CHBr(COOH)_2$, 0.09 M; $CH_2(COOH)_2$, 0.05 M; and Fe(1,10-phenanthroline)$_3$, 3.4 mM. The obstacle is colorless with a dark band at the edges resulting from the change of refraction index from silicon oil to agarose gel. The photographs were taken from a video screen at ~30-s intervals (**A** to **F**) and show a 28 mm by 25 mm section of the reactive layer. Period of stimulation was 70 s, and period of the spiral wave was 89.5 s.

reaction (*12*). As with the agarose gel, the reaction sheet in the millipore filter was covered with a 2-mm layer of silicon oil. Again, when the frequency of the wave train exceeded a critical value, a spiral wave was created (Fig. 3, B and C). In time, new spirals appeared at the corner (Fig. 3, C and D). When the wave source at the bottom was subsequently removed, the spiral wave remained close to the corner (Fig. 3, E and F).

The mechanism of rotor generation described in this report is related to the curvature effect on the propagation of waves in excitable media (*13*). The velocity of the wave decreases with increased curvature of the front and can become zero and even negative if the curvature is high enough. The main effect of the obstacle is to break the wave into two waves, which will either go around the obstacle while remaining attached to the boundary (Fig. 1B) or form two free ends (Fig. 1C). Once the break is formed, curvature at the tip is large and will impede the progress of the wave around a corner. According to (*14*) there are two types of behavior of a wave break depending on the excitability of the medium: In media with high excitability, the wave break expands into the unexcited medium, whereas in media with low excitability it contracts. The high frequency of external stimulation has the effect of decreasing the excitability of the medium and, hence, if the frequency is high, the wave break contracts rather than expands and the re-entrant pattern may be generated (*15*). Notice that for free wave tips to be created, the boundary must have high curvature, as a wave break will not separate from a slowly curving boundary. It is also necessary to have a large turning angle at the corner. If the turning angle is small, the wave may separate from the corner but will have insufficient room to make the first rotation, as it will collide and reconnect with the boundary. At present, there is no adequate quantitative theory describing this phenomenon.

The geometry of the medium necessary for the spiral wave origination is general: There must be corners with sufficient sharpness, and the frequency of incoming waves must be supercritical. These conditions are easily met in many of the known active media, such as heart, growing amoebae populations, and reactive solutions that propagate catalytic waves. For heart tissue, the role of a sharp corner may be played by fiber branching or by a myocardial infarction that serves as the obstacle around which the re-entrant pattern is generated. The separation of the wave from the boundary of an obstacle is important in

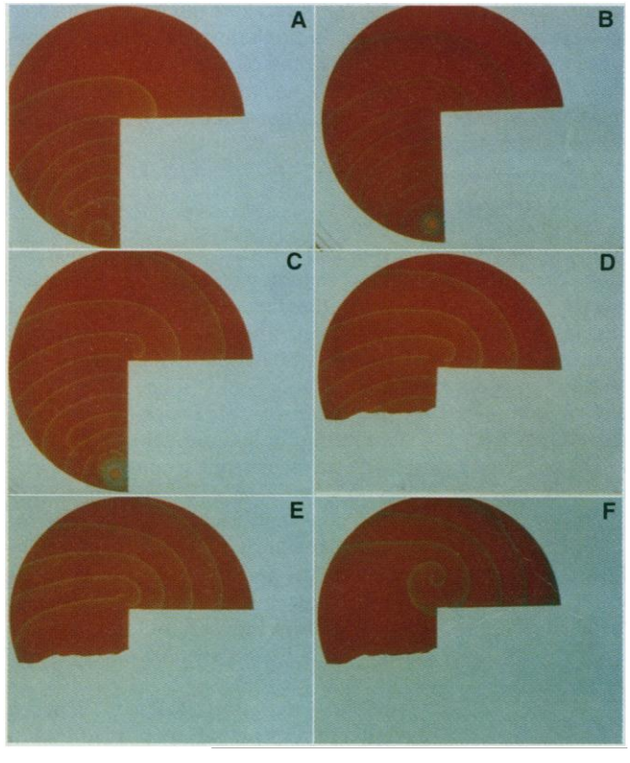

Fig. 3. (**A** to **F**) The complete sequence of events showing spiral wave creation in a piece of millipore filter paper soaked with BZ reagent. In (B), a drop of 0.15 M sulfuric acid serves as a high-frequency pacemaker (spot at bottom of the filter). The pacemaker is removed in (D), (E), and (F). The diameter of the millipore filter is 45 mm. Time intervals between frames: 5 min (A and B), 4 min (B and C), 1.5 min (C and D), 6 min (D and E), and 4 min (E and F).

other contexts in excitable media such as autowave diffraction (*16*).

REFERENCES AND NOTES

1. A. T. Winfree, *Science* **175**, 634 (1972).
2. K. I. Agladze and V. I. Krinsky, *Nature* **292**, 424 (1982).
3. G. Gerisch, *Naturwissenschaften* **58**, 430 (1971); F. Siegert and C. J. Weijer, *Proc. Natl. Acad. Sci. U.S.A.* **89**, 6433 (1992).
4. A. Gorelova and J. Bures, *J. Neurobiol.* **14**, 353 (1983).
5. M. A. Alessie, F. I. M. Bonke, F. J. G. Schopman, *Circ. Res.* **33**, 54 (1973); J. M. Davidenko, A. M. Pertsov, R. Salomontsz, W. Baxter, J. Jalife, *Nature* **355**, 349 (1991); J. M. Davidenko, P. F. Kent, D. R. Chialvo, D. C. Michaels, J. Jalife, *Proc. Natl. Acad. Sci. U.S.A.* **87**, 8785 (1990).
6. G. Dupont and A. Goldbeter, *BioEssays* **14**, 1 (1992); J. Lechleiter, S. Girard, E. Peralta, D. Clapham, *Science* **252**, 123 (1991).
7. A. N. Zaikin and A. M. Zhabotinsky, in *Oscillatory Processes in Biological and Chemical Systems*, E. E. Sel'kov, Ed. (Nauchnii Center Biologicheskih Issledavanii, Pushchino, USSR, 1971), vol. 2, p. 79.
8. H. H. Rotermund, W. Engel, M. Kordesch, G. Ertl, *Nature* **343**, 355 (1990).
9. K. I. Agladze, V. I. Krinsky, A. M. Pertsov, *ibid.* **308**, 834 (1984).
10. G. K. Moe, W. C. Rheinboldt, J. A. Abildskov, *Am. Heart J.* **67**, 200 (1964).
11. V. I. Krinsky and K. I. Agladze, *Physica D* **8**, 50 (1983).
12. A. T. Winfree, *Theor. Chem.* **4**, 1 (1978).
13. J. P. Keener, *J. Math. Biol.* **29**, 629 (1991).
14. A. M. Pertsov, A. V. Panfilov, F. U. Medvedeva, *Biofizica* **28**, 100 (1983).
15. A. T. Winfree, *Appl. Mech. Rev.* **43**, 297 (1990).
16. A. M. Pertsov, E. A. Ermakova, E. E. Shnol, *Physica D* **44**, 178 (1990).
17. A. V. Panfilov and A. M. Pertsov, *Dokl. Akad. Nauk SSSR* **274**, 1500 (1984).

18. For computations we used Fitz-Hugh Nagumo–type equations with piecewise linear "Pushchino kinetics" (*17*).

$$\partial e/\partial t = \nabla^2 e - f(e) - g$$
$$\partial g/\partial t = \epsilon(e)(ke - g) \quad (1)$$

with $f(e) = C_1 * e$ when $e < e_1$; $f(e) = -C_2 * e + a$ when $e_1 \le e \le e_2$; $f(e) = C_3 * (e - 1)$ when $e > e_2$; and $\epsilon(e) = \epsilon_1$ when $e < e_1$; $\epsilon(e) = \epsilon_2$ when $e_1 \le e \le e_2$; $\epsilon(e) = \epsilon_3$ when $e > e_2$. The parameters determining the shape of the function $f(e)$ are $e_1 = 0.0065$, $e_2 = 0.841$, $\epsilon_1 = 0.14$, $\epsilon_2 = 0.059$, $\epsilon_3 = 2.5$, $C_1 = 20$, $C_2 = 3$, $C_3 = 15$, $a = 0.15$, and $k = 3$. With these parameter values, the function $f(e)$ is continuous. To integrate Eq. 1, we used the explicit Euler method with time step $ht = 0.01$ and space step $hx = 0.3$, which gives less than 4% error for the velocity of plane wave propagation and 7% error for the period of the spiral rotation, about 15.5 time units. Neumann boundary conditions were used. A rectangular inexcitable obstacle was made using Neumann boundary conditions at its edges. External high-frequency stimulation was applied at one edge of the excitable medium with stimuli having amplitude four times the threshold value.

23 December 1993; accepted 13 April 1994

High-Resolution Nuclear Magnetic Resonance Spectroscopy in a Circularly Polarized Laser Beam

A. D. Buckingham and L. C. Parlett

Nuclei in a fluid subjected to a continuous wave circularly polarized light beam are predicted to experience a static magnetic field proportional to $\mathbf{E}^{\pm} \times \dot{\mathbf{E}}^{\pm}$, where $\mathbf{E}^{\pm}$ is the electric vector of the right or left circularly polarized wave and the dot denotes a time derivative. The field strongly depends on the local electronic structure and is present in all atoms. For an intensity of 10 watts per square centimeter propagating in the direction of the field of a magnetic resonance spectrometer, the general theory presented here predicts shifts of $\pm 4 \times 10^{-8}$ hertz for protons and $\pm 10^{-5}$ hertz for fluorine-19. Larger shifts are predicted if the laser frequency is near an optical absorption.

Recently, there has been interest in laser-enhanced nuclear magnetic resonance (NMR) spectroscopy (*1–3*). Evans (*1*) predicted that a circularly polarized laser beam could raise NMR frequencies dramatically. Warren *et al.* (*2*) studied solutions of the chiral molecule *p*-methoxyphenyliminocamphor in linearly polarized as well as left and right circularly polarized light of wavelength 514 nm; they observed bulk high-field shifts on the order of 0.01 part per million and smaller differential shifts. Harris and Tinoco (*3*) estimated the change in the chemical shift of a nucleus induced by a polarized laser beam and concluded it was far too small to be measured.

Department of Chemistry, University of Cambridge, Lensfield Road, Cambridge CB2 1EW, UK.

Evans believes that a circularly polarized beam has an associated static magnetic field parallel to the direction of propagation and proportional to the square root of the intensity (*4, 5*), but this would lead to huge NMR shifts and would violate charge conjugation symmetry (*6*). Evans (*5*) also considers a second-order interaction of the laser with the molecular antisymmetric polarizability $\alpha'_{\alpha\beta} = -\alpha'_{\beta\alpha}$, but he apparently failed to appreciate that in NMR spectroscopy, it is the antisymmetric polarizability induced by the nuclear magnetic moment that is relevant, just as it is the antisymmetric polarizability induced by the magnetostatic field that is responsible for the Faraday effect (*7*).

We show that the NMR shift may be expressed in terms of $\alpha'_{\alpha\beta}$ perturbed by the nuclear magnetic moment. Warren *et al.* (*2, 8*) suggest that the polarization proportional to the electric field of the light wave could produce a magnetic field at a nucleus, but presumably this field would be oscillating at the optical frequency and therefore would have no first-order effect on the spectrum. Harris and Tinoco (*3, 9*) consider nonchiral changes in energy proportional to the product $I_0 B_z^{(0)}$, where I_0 is the intensity of the laser beam and $B_z^{(0)}$ the magnetic field of the NMR spectrometer; they also consider small, chirally sensitive shifts proportional to I_0 and $I_0 B_z^{(0)}$.

In this report, we show that the electrons of any molecule in a circularly polarized light beam acquire a mean time-independent current density proportional to $\mathbf{E}^{\pm} \times \dot{\mathbf{E}}^{\pm}$, where $\mathbf{E}^{\pm}$ is the electric field associated with a right (+) or left (−) circularly polarized light wave and the dot denotes differentiation with respect to time. This current produces a magnetic moment [this is known as the inverse Faraday effect (*10*)] as well as a magnetic field at each nucleus. A steady molecular current induced by an optical field must be an even function of the field strength $|\mathbf{E}|$ in order that it be time-independent and an odd function of $\dot{\mathbf{E}}$ in a diamagnetic molecule in order that it should have the temporal properties of a current.

The electric field of a circularly polarized plane wave propagating in the direction of the unit vector $\mathbf{k}$, the z direction, is

$$\mathbf{E}^{\pm} = \frac{1}{\sqrt{2}} E^{(0)} \left[\mathbf{i} \cos \omega\left(t - \frac{nz}{c}\right) \mp \mathbf{j} \sin \omega\left(t - \frac{nz}{c}\right)\right] \quad (1)$$

where $\mathbf{i}$ and $\mathbf{j}$ are unit vectors in the x and y directions, n is the refractive index, c the velocity of light in vacuo, and ω the angular frequency. The intensity of the beam is

$$I_0 = \frac{1}{2} \epsilon_0 [E^{(0)}]^2 c \quad (2)$$

where ϵ_0 is the permittivity of free space and I_0 is the power per unit area of a parallel beam of light; if $I_0 = 1$ W/cm^2, $E^{(0)} = 27.4$ V/cm.

From Eq. 1, the time derivative of $\mathbf{E}^{\pm}$ is

$$\dot{\mathbf{E}}^{\pm} \equiv \frac{\partial \mathbf{E}^{\pm}}{\partial t} = -\frac{\omega}{\sqrt{2}} E^{(0)} \left[\mathbf{i} \sin \omega\left(t - \frac{nz}{c}\right) \pm \mathbf{j} \cos \omega\left(t - \frac{nz}{c}\right)\right] \quad (3)$$

The vector product $\mathbf{E}^{\pm} \times \dot{\mathbf{E}}^{\pm} = \mp(\omega/2)[E^{(0)}]^2 \mathbf{k}$ is time-independent and behaves under the operations of parity P (that is, inversion of the coordinates of all particles through the origin, including the sources of the applied fields) and time reversal T (that